

# $\text{Na}_{2.8}\text{Cu}_5\text{Sn}_{5.6}$ : A Crystalline Alloy Featuring Intermetalloid $^1_\infty\{\text{Sn}_{0.6}\text{@Cu}_5\text{@Sn}_5\}$ Double-Walled Nanorods with Pseudo-Five-Fold Symmetry\*\*

Saskia Stegmaier and Thomas F. Fässler\*

In crystalline materials true five-fold symmetry is realized only by quasicrystals as it is not compatible with translational symmetry.<sup>[1–3]</sup> Local (pseudo-)five-fold symmetry, however, is feasible if it does not extend through the whole crystal. For molecular crystals with discrete molecular units and weak intermolecular interactions this is easily realized and occurs frequently, but it can also be found in extended solid-state structures of alloys, especially in form of icosahedral or pentagonal dodecahedral arrangements. Furthermore, among intermetallics there are, for example, approximants to icosahedral quasicrystals<sup>[4]</sup> that show building blocks in which, starting from one site, the icosahedral building principle “radially” propagates through several structural shells.

The coexistence of different bonding characteristics in alloys is a peculiarity of the Zintl phases that are composed of an electropositive metal *A* and a more electronegative p-block (semi)metal *E*. Within the Zintl concept, complete electron transfer from *A* to *E* is formally assumed, and the Zintl phases can be understood as *saltlike* compounds with cations of *A* and (poly)anions of *E*. For the classic Zintl phases the atoms of the polyanions are covalently connected according to the basic 8–*N* rule. Discrete deltahedral cage cluster polyanions can be rationalized using the Wade–Mingos rules. In this view  $[\text{Sn}_9]^{4-}$  anions in  $\text{K}_4\text{Sn}_9$ ,<sup>[5]</sup> for example, represent *nido* clusters. These concepts can also be seen to cover some intermetallic phases with discrete anionic cage clusters of group 13 elements with single endohedral d-block metal atoms.<sup>[6]</sup> Until recently such a general concept was, however, not recognized for intermetallic compounds with a high d-block metal (*T*) content. With the  $\text{A}_{12}\text{Cu}_{12}\text{Sn}_{21}$  (*A* = Na, K, Rb, Cs) phases,<sup>[7]</sup> we lately found examples of such polar intermetallic compounds that feature more complex *T–E* cluster polyanions with a multiply endohedral structure: onion-skin-like  $\{\text{Sn@Cu}_{12}\text{@Sn}_{20}\}$  clusters which are separated by *A* atoms. A saltlike description with discrete intermetalloid<sup>[8]</sup>  $[\text{Sn@Cu}_{12}\text{@Sn}_{20}]^{12-}$  anions is in accord with the results of theoretical calculations.<sup>[7]</sup>

Here we now present the ternary phase  $\text{Na}_{2.8}\text{Cu}_5\text{Sn}_{5.6}$  which features discrete one-dimensional Cu–Sn columns  $^1_\infty\{\text{Sn}_{0.6}\text{@Cu}_5\text{@Sn}_5\}$  with pseudo-pentagonal symmetry that show a composition with an almost equal ratio of Cu to Sn. The Cu–Sn wires are aligned parallel, associated with a highly anisotropic band structure and indicating one-dimensional metallic behavior.

$\text{Na}_{2.8}\text{Cu}_5\text{Sn}_{5.6}$  was obtained by the reaction of elemental Na with a preformed Cu–Sn alloy. The phase forms needle-shaped crystals which can appear in bundles (Figure 1). In the orthorhombic crystal structure of  $\text{Na}_{2.78(4)}\text{Cu}_5\text{Sn}_{5.62(1)}$  discrete  $^1_\infty\{\text{Sn}_{0.6}\text{@Cu}_5\text{@Sn}_5\}$  rods are separated by Na atoms and are

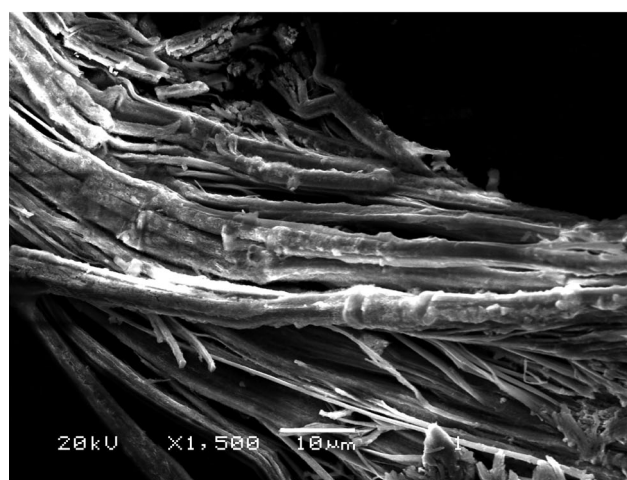
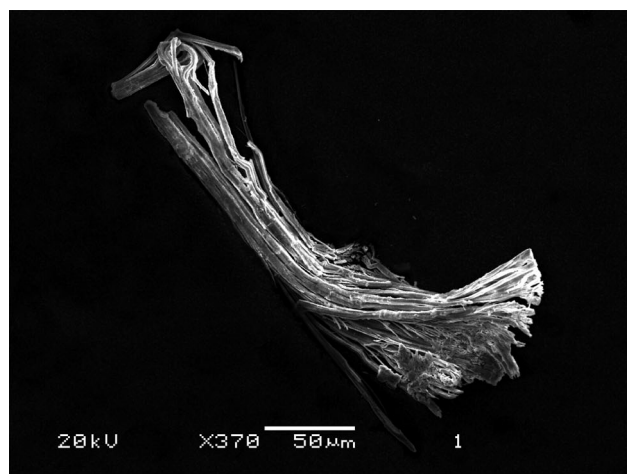


**Figure 1.** SEM images showing a bundle of fibrous (needle-shaped) crystals of  $\text{Na}_{2.8}\text{Cu}_5\text{Sn}_{5.6}$ .

[\*] Dipl.-Chem. S. Stegmaier, Prof. Dr. T. F. Fässler  
Department of Chemistry, Technische Universität München  
Lichtenbergstrasse 4, 85747 Garching (Germany)  
E-mail: thomas.faessler@lrz.tum.de

[\*\*] We thank R. Brimiouille for synthetic work, M.B. Boeddinghaus and I. Werner for SQUID measurements, and A. Hoffmann for taking the SEM pictures. S.S. would also like to thank the Studienstiftung des Deutschen Volkes for a PhD fellowship.

Supporting information for this article is available on the WWW under <http://dx.doi.org/10.1002/anie.201107985>.

arranged in style of a hexagonal rod packing (Figure 2b). The  ${}^1_{\infty}\{\text{Sn}_{0.6}@\text{Cu}_5@\text{Sn}_5\}$  Cu–Sn columns show an outer shell of Sn atoms enclosing an inner tube of Cu atoms (Figure 2a) and Sn atoms situated on the central column axis with disorder (Figure 2d). The double-walled Cu–Sn tubes arise from the staggered stacking of planar  $\{\text{Cu}_5\text{Sn}_5\}$  units made of  $\{\text{Cu}_5\}$  pentagons with all edges capped by Sn atoms (Figure 2c).

The Cu–Cu distances in  $\text{Na}_{2.8}\text{Cu}_5\text{Sn}_{5.6}$  are between 2.572(1) and 2.879(2) Å. The range includes that for the  $\{\text{Sn}@\text{Cu}_{12}@\text{Sn}_{20}\}$  clusters<sup>[7]</sup> and fits in with that for intermetallic phases like  $\text{Ca}_3\text{Cu}_8\text{Sn}_4$  and  $\text{CaCu}_9\text{Sn}_4$ .<sup>[9]</sup> The distances between the Sn atoms of the outer shell and the Cu atoms lie between 2.661(1) and 2.789(1) Å, in the same range as the Cu–Sn distances in binary Cu–Sn bronzes (e.g. 2.631 to 2.860 Å in  $\eta'$ - $\text{Cu}_6\text{Sn}_5$ <sup>[10]</sup>), and matching those in the  $\{\text{Sn}@\text{Cu}_{12}@\text{Sn}_{20}\}$  clusters.<sup>[7]</sup> The intracolumn Sn–Sn distances of 3.317(1) to 3.400(1) Å are significantly longer than the distances in metallic  $\beta$ -Sn (3.016 and 3.175 Å), but they are much shorter than the shortest intercolumn Sn–Sn distances of 4.928(1) Å, which clearly allows to designate the columns as separated from each other.

The atoms in the center of the Cu–Sn columns are disordered, and a structure model with two partially occupied Sn sites was used to account for this (see Figure 2d and the Supporting Information). The freely refined occupancy factors for these sites are 0.26(1) for Sn4 and 0.18(1) for Sn5. No indication for a superstructure was evident.

Each planar  $\{\text{Cu}_5\text{Sn}_5\}$  unit is surrounded by six Na sites in the same plane (Figure 2c) breaking the pseudo-five-fold symmetry. Free refinement of the occupancy parameters for the Na1 and Na2 sites led to values of 0.93(2) and 0.92(2), respectively. The shortest Na–Sn and Na–Na distances are 3.147(4) Å and 3.73(1) Å, respectively.

The “ ${}^1_{\infty}\{\text{Sn}_{1.2}@\text{Cu}_{10}@\text{Sn}_{10}\}$ ” column in “ $\text{Na}_{11.2}\text{Cu}_{20}\text{Sn}_{22.4}$ ” is closely related to the  $\{\text{Sn}@\text{Cu}_{12}@\text{Sn}_{20}\}$  cluster in the  $\text{A}_{12}\text{Cu}_{12}\text{Sn}_{21}$  phases,<sup>[7]</sup> which is comprised of a  $\{\text{Sn}_{20}\}$  pentagonal dodecahedron surrounding a  $\{\text{Cu}_{12}\}$  icosahedron with a single Sn atom in the center (Figure 2h). The pentagonal antiprismatic  $\{\text{Sn}@\text{Cu}_{10}@\text{Sn}_{10}\}$  cluster fragment as highlighted in Figure 2h bears an obvious resemblance to the segment of the column shown in Figure 2g.

Electronic structure calculations (TB-LMTO-ASA<sup>[11]</sup>) were performed for a model  $\text{Na}_3\text{Cu}_5\text{Sn}_{5.5}$  assuming an ordered structure with Sn atoms at the center of every second pentagonal antiprismatic void in the columns, and with full occupancy of the Na positions (see the Supporting Information). The high anisotropy of the calculated band structure (see Figure 3 and the Supporting Information) confirms the description of the phase as a “metal in one dimension”. Along directions that correspond to the orientation of the column axes ( $\Gamma \rightarrow \text{Y}$  in Figure 3) bands with large dispersion occur, and steep bands cross the Fermi level ( $E_F$ ). In contrast, flat bands and band gaps are found along lines corresponding to directions perpendicular to the wires (shaded light gray in Figure 3). Along some of those lines rather flat bands cross  $E_F$  for the  $\text{Na}_3\text{Cu}_5\text{Sn}_{5.5}$  model (upper dotted line at 0 eV in Figure 3). Lowering of  $E_F$  by about 0.2 eV opens a band gap along the directions perpendicular to the tubes (lower dotted line and shaded dark gray in Figure 3, respectively) along all

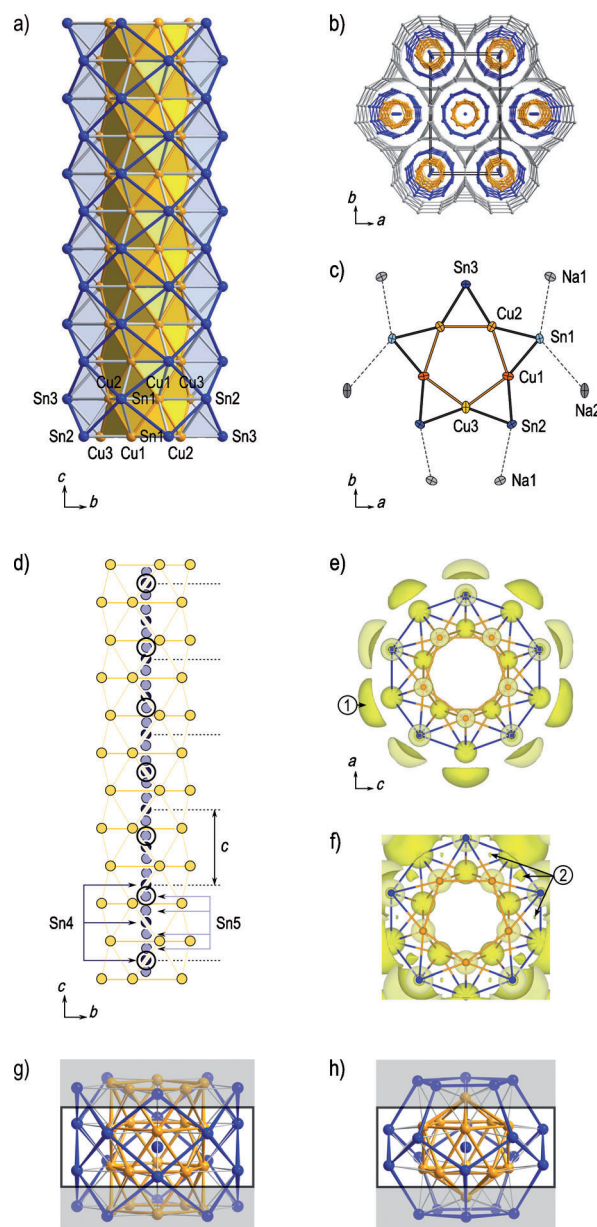


**Figure 2.** a) Double-walled Cu–Sn tube. b) Cu–Sn columns separated by Na atoms in  $\text{Na}_{2.8}\text{Cu}_5\text{Sn}_{5.6}$ . Contacts between Cu (orange) and Sn (blue) atoms not shown for clarity, gray lines illustrate the Na substructure. c) Coplanar  $\{\text{Cu}_5\text{Sn}_5\}$  unit with surrounding Na sites. Thermal ellipsoids at 70% probability level. d) Model with sites Sn4 and Sn5 used to account for the disorder of the Sn atoms in the center of the double-walled tube. Cu atoms (orange) shown, outer Sn atoms omitted. Black circles indicate a possible pattern with one out of five positions occupied leading to the composition  ${}^1_{\infty}\{\text{Sn}_{0.6}@\text{Cu}_5@\text{Sn}_5\}$ . e) and f) ELF isosurface representations. e) Lone-pair-like basins (1) at the outer Sn atoms, isovalue 0.60. f) Calculation for a model  $\text{Na}_3\text{Cu}_5\text{Sn}_{5.5}$  with Cu–Sn columns running along  $b$ . Basins (2) are indicative for multicenter Cu–Sn interactions, isovalue 0.37. g) and h) Cu–Sn columns and clusters in ternary A–Cu–Sn phases. g)  ${}^1_{\infty}\{\text{Sn}_{0.6}@\text{Cu}_5@\text{Sn}_5\}$  column in  $\text{Na}_{2.8}\text{Cu}_5\text{Sn}_{5.6}$ . Only one Sn4 site in the column center shown. h)  $\{\text{Sn}@\text{Cu}_{12}@\text{Sn}_{20}\}$  cluster in  $\text{A}_{12}\text{Cu}_{12}\text{Sn}_{21}$  (A = Na, K, Rb, Cs).<sup>[7]</sup> Cu and Sn atoms shown as orange and blue spheres, respectively.

those lines. Within a rigid band model a lowering of  $E_F$  is achieved through a lower Na content, and the calculated

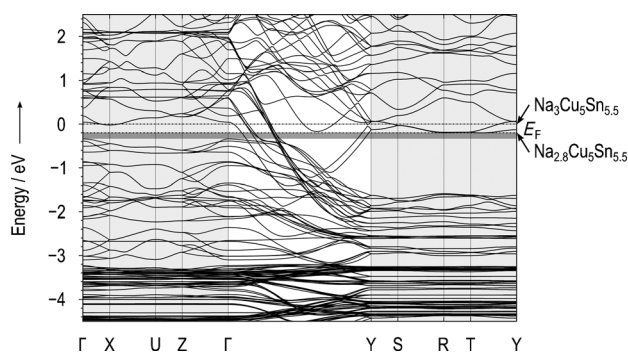


**Figure 3.** a) Band structure calculated for a model  $\text{Na}_3\text{Cu}_5\text{Sn}_{5.5}$ .  $\Gamma \rightarrow \text{Y}$  corresponds to the orientation of the Cu–Sn columns (running along  $b$  for the model structure).

integrated density of states (IDOS) value at  $-0.2$  eV for the  $\text{Na}_3\text{Cu}_5\text{Sn}_{5.5}$  model correlates to the approximate composition  $\text{Na}_{2.8}\text{Cu}_5\text{Sn}_{5.5}$ . This corresponds to the crystal structure refinement with partially occupied Na sites resulting in a composition of  $\text{Na}_{2.78(4)}\text{Cu}_5\text{Sn}_{5.62(1)}$ . Representations of the electron localization function (ELF) are dominated by lone-pair-type valence basins at the Sn atoms of the outer column shell (①), but also show multicenter interactions (②) within the intermetallic Cu–Sn rods (see Figure 2 e,f and the Supporting Information). Electron localization in lone pairs has been described for other “confined metals”,<sup>[12]</sup> and the shell of outward pointing lone pairs also shows the close relationship of the columns to discrete Zintl anion clusters of group 14 elements.<sup>[13]</sup> The occurrence of lone pairs localized at Sn atoms is a generally known feature of intermetallic stannides.<sup>[14–17]</sup>

Due to the occurrence of small amounts of  $\text{NaSn}_2$  as by-product (powder pattern shown in the Supporting Information), the determination of properties of the bulk sample cannot be unambiguously achieved. Contacting an individual crystal for conductivity measurements is hampered by their fibrous structure.

The new  $A\text{--Cu--Sn}$  phases provide further links between different fields of solid-state and cluster chemistry and thus allow a comprehensive view: A counterpart to  $[\text{Sn@Cu}_{12}\text{@Sn}_{20}]^{12-}$  is known in form of the iso-(valence)electronic and isostructural  $[\text{As@Ni}_{12}\text{@As}_{20}]^{3-}$ <sup>[18]</sup> cluster anion that was prepared from  $[\text{As}_7]^{3-}$  Zintl ion solutions,<sup>[18]</sup> and the polycationic  ${}^1_{\infty}\{\text{Bi}_{0.6}\text{@Ni}_5\text{@Bi}_5\}$  rods in the subhalide  $\text{Bi}_{5.6}\text{Ni}_5\text{I}^{[19]}$  are—albeit not as clearly separated from each other—closely related and isostructural to the polyanionic  ${}^1_{\infty}\{\text{Sn}_{0.6}\text{@Cu}_5\text{@Sn}_5\}$  columns in  $\text{Na}_{2.8}\text{Cu}_5\text{Sn}_{5.6}$ . The recent synthesis of the metastable  $\text{Bi}_{28}\text{Ni}_{25}$  by reduction of  $\text{Bi}_{5.6}\text{Ni}_5\text{I}^{[20]}$  further corroborates the close relation between intermetallic polyions and intermetallic compounds. Whether an oxidation of  $\text{Na}_{2.8}\text{Cu}_5\text{Sn}_{5.6}$  might lead to a binary Cu–Sn phase with Cu–Sn columns is currently under investigation.

Discrete double-walled pentagonal antiprismatic cluster columns, first reported for  $\text{Ta}_6\text{Te}_5$ ,<sup>[21,22]</sup> are exceptionally rare and also only few discrete heterometallic ionic cluster columns are known. The double-walled square antiprismatic  ${}^1_{\infty}\{\text{S@Ni}_8\text{@Bi}_8\}$  columns in  $\text{Ni}_8\text{Bi}_8\text{Si}^{[23]}$  and  $\text{Ni}_8\text{Bi}_8\text{Si}_2^{[24]}$

include S, thus they are not exclusively built of (semi)metallic elements. Smaller single-walled anionic tubes built of Tl atoms with pentagonal antiprismatic voids filled with Cd occur in  $\text{A}_5\text{Cd}_2\text{Tl}_{11}$  ( $A = \text{Cs}, \text{Rb}$ ).<sup>[25]</sup>

The conceptual treatment of ternary polar intermetallic phases comprised of an electropositive metal  $A$ , a late d-block metal  $T$ , and a p-block (semi)metal  $E$  often involves the Zintl concept, starting the discussion with the binary  $A\text{--}E$  Zintl phases and considering a substitution of  $E$  with  $T$ . This is often valuable especially if the  $E:T$  ratio is high. For the new  $A\text{--Cu--Sn}$  phases with a rather high Cu content the complementary view starting with a  $T\text{--}E$  alloy is possibly more insightful. The reaction of an alkali metal  $A$  with a Cu–Sn alloy may be seen to parallel the formation of a Zintl phase by the reduction of a more electronegative (semi)metal with an electropositive metal. And in analogy to the Zintl phases the new  $A\text{--Cu--Sn}$  phases represent saltlike intermetallic compounds with alkali-metal cations and polyanions. But while the structure and bonding of the (poly)anionic part (comprised of p-block element atoms) in the classic Zintl phases can be rationalized with concepts such as the  $8-N$  rule or the Wade–Mingos rules, the situation is more complex for the Cu–Sn polyanions in the  $A\text{--Cu--Sn}$  phases—just as the concepts for p-block elements with covalent bonding strongly differ from those for metallic binary alloys. The discrete intermetallic Cu–Sn cluster polyanions in  $\text{A}_{12}\text{Cu}_{12}\text{Sn}_{21}$  feature delocalized cluster bonding and the discrete Cu–Sn rods in  $\text{Na}_{2.8}\text{Cu}_5\text{Sn}_{5.6}$  give rise to quasi-one-dimensional metallic bonding characteristics.

## Experimental Section

All details on the synthesis, SEM, EDX, and SQUID measurements, single-crystal and powder XRD analysis, and computational studies are provided in the Supporting Information. Selected crystallographic data:  $\text{Na}_{2.78(4)}\text{Cu}_5\text{Sn}_{5.62(1)}$ ,  $Cmcm$  (No. 63),  $a = 13.008(1)$  Å,  $b = 22.389(1)$  Å,  $c = 4.1852(3)$  Å,  $V = 1218.9(2)$  Å<sup>3</sup>,  $Z = 4$ ;  $\rho_{\text{calc}} = 5.71$  g cm<sup>−3</sup>;  $wR_2(\text{all data}) = 0.054$ . Further details on the crystal structure investigations may be obtained from the Fachinformationszentrum Karlsruhe, 76344 Eggenstein-Leopoldshafen, Germany (fax: (+49) 7247-808-666; e-mail: crysdata@fiz-karlsruhe.de), on quoting the depository number CSD-423645. Calculations were performed for a model  $\text{Na}_3\text{Cu}_5\text{Sn}_{5.5}$  in space group  $Pnmm$  (No. 58), with  $a = 22.3892$  Å,  $b = 4.1852$  Å, and  $c = 13.0075$  Å.

Received: November 13, 2011

Published online: February 1, 2012

**Keywords:** bronze · copper · nanowires · solid-state structures · stannides

- [1] D. Shechtman, I. Blech, D. Gratias, J. W. Cahn, *Phys. Rev. Lett.* **1984**, *53*, 1951.
- [2] D. Levine, P. J. Steinhardt, *Phys. Rev. Lett.* **1984**, *53*, 2477.
- [3] *Quasicrystals: Structure and Physical Properties* (Ed.: H.-R. Trebin), Wiley-VCH, Weinheim, **2003**.
- [4] A. I. Goldman, R. F. Kelton, *Rev. Mod. Phys.* **1993**, *65*, 213.
- [5] C. Hoch, M. Wendorff, C. Röhr, *Acta Crystallogr. Sect. C* **2002**, *58*, i45.
- [6] J. D. Corbett, *Angew. Chem.* **2000**, *112*, 682; *Angew. Chem. Int. Ed.* **2000**, *39*, 670.
- [7] S. Stegmaier, T. F. Fässler, *J. Am. Chem. Soc.* **2011**, *133*, 19758.



- [8] T. F. Fässler, S. D. Hoffmann, *Angew. Chem.* **2004**, *116*, 6400; *Angew. Chem. Int. Ed.* **2004**, *43*, 6242.
- [9] M. Pani, F. Merlo, M. L. Fornasini, *Z. Anorg. Allg. Chem.* **2007**, *633*, 1581.
- [10] A. K. Larsson, L. Stenberg, S. Lidin, *Acta Crystallogr. Sect. B* **1994**, *50*, 636.
- [11] *The Stuttgart TB-LMTO-ASA Program (Version 4.7)*, O. Jepsen, A. Burkhardt, O. K. Andersen, Max-Planck-Institut für Festkörperforschung, Stuttgart, **1998**.
- [12] M. Ruck, *Z. Kristallogr.* **2010**, *225*, 167.
- [13] S. Scharfe, F. Kraus, S. Stegmaier, A. Schier, T. F. Fässler, *Angew. Chem.* **2011**, *123*, 3712; *Angew. Chem. Int. Ed.* **2011**, *50*, 3630.
- [14] T. F. Fässler, *Chem. Soc. Rev.* **2003**, *32*, 80.
- [15] T. F. Fässler, S. Hoffmann, C. Kronseder, *Z. Anorg. Allg. Chem.* **2001**, *627*, 2486.
- [16] T. F. Fässler, *Z. Anorg. Allg. Chem.* **1998**, *624*, 569.
- [17] T. F. Fässler, C. Kronseder, *Angew. Chem.* **1997**, *109*, 2800; *Angew. Chem. Int. Ed. Engl.* **1997**, *36*, 2683.
- [18] M. J. Moses, J. C. Fettingner, B. W. Eichhorn, *Science* **2003**, *300*, 778.
- [19] M. Ruck, *Z. Anorg. Allg. Chem.* **1995**, *621*, 2034.
- [20] M. Kaiser, A. Isaeva, M. Ruck, *Angew. Chem.* **2011**, *123*, 6302; *Angew. Chem. Int. Ed.* **2011**, *50*, 6178.
- [21] M. Conrad, B. Harbrecht, *J. Alloys Compd.* **1992**, *187*, 181.
- [22] M. Conrad, Dissertation, Universität Dortmund, **1997**.
- [23] A. I. Baranov, L. Kloos, A. V. Olenov, B. A. Popovkin, A. I. Romanenko, A. V. Shevelkov, *J. Am. Chem. Soc.* **2001**, *123*, 12375.
- [24] A. I. Baranov, L. Kloos, A. V. Olenov, B. A. Popovkin, A. I. Romanenko, *Inorg. Chem.* **2003**, *42*, 3988.
- [25] S. Kaskel, J. D. Corbett, *Inorg. Chem.* **2000**, *39*, 3086.